CHAPITRE 5. Influence of the pore structure of wood on moisture desorption at high relative humidities

5.1 Résumé

L'influence de la structure poreuse du bois sur la courbe de désorption a été étudiée pour deux espèces tempérées et cinq tropicales. Deux techniques expérimentales ont été utilisées pour effectuer des tests de désorption à partir de la saturation intégrale à 25°C. La première utilise des solutions salines saturées (valeurs échelonnées de 33% à 90 % d'humidité relative) tandis que la seconde utilise la membrane poreuse sous pression (au-dessus de 96% d'humidité relative). Dans ce travail, notre attention est portée plus particulièrement sur les résultats obtenus à hautes valeurs d'humidité relative, domaine dans lequel la désorption est contrôlée par les forces capillaires. La structure poreuse de ces espèces feuillues a été caractérisée par porosimétrie au mercure et par anatomie quantitative. Les résultats montrent que la désorption de l'eau liquide dépend fortement de l'espèce. La porosimétrie au mercure est une technique importante pour évaluer le cheminement du fluide dans le bois, ce qui permet de prédire le comportement en désorption pour de fortes valeurs d'humidité relative. Les résultats d'anatomie quantitative permettent de prédire le premier pic lié aux vaisseaux.

5.2 Abstract

The influence of the pore structure on moisture desorption of two temperate and five tropical hardwoods was studied. Two experimental techniques were used to perform moisture desorption tests from full saturation at 25ºC. The first one was the saturated salt solutions (between 33% and 90% relative humidity) and the second one was the pressure membrane method (above 96% relative humidity). More emphasis was given to results obtained at high relative humidities, given that sorption in that case is mainly governed by the capillary forces. The porous structure of these hardwoods was characterized by mercury intrusion porosimetry (MIP) and by quantitative anatomical analysis. The results showed that desorption of liquid water was very different among the hardwood species. MIP technique appeared as an important tool to evaluate the fluid paths within wood, which permitted the prediction of water behavior in wood during drainage from full saturation at

high relative humidities. Quantitative anatomical results were very useful for explaining the first steps of drainage and mercury penetration in wood.

5.3 Introduction and background

The knowledge of the capillary system is very important for studying the movement of fluids and vapors through a porous material. Wood is a material constituted by a heterogeneous porous medium. This fact influences its sorption properties, especially at high relative humidities (RH), where equilibrium is mainly controlled by the capillary forces and consequently by the microstructure of wood species.

The anatomical parameters of wood present a large variability among species. For example, vessel proportion in temperate hardwoods is approximately 30% with a range from 6.5 to 55% (Panshin and de Zeeuw 1980). The proportion of fibers may account for 20% to 70% of wood volume depending on species. Axial parenchyma makes up 1% to 18% of the volume of temperate woods, but this may reach 50% in tropical woods. Ray parenchyma may include 5% to 30% of the volume of temperate woods (Siau 1995). As a result, the porous structure of wood can vary within a wide range (from cell wall cavities as smaller as 0.0015 μm in radius to vessels larger than 100 μm). This complex structure largely affects the wood - water relationships, in particular at high RH values.

The present study uses the water potential concept (ψ) to describe the energy state of water in wood (Fortin 1979; Cloutier and Fortin 1991; Defo et al. 1999). This concept can be theoretically applied to water in wood independently of its state (liquid, vapor or bound water). An advantage in applying this concept is that when the moisture content (MC) - ψ relationship is plotted, the region between 96% and 100% RH is widely spread out. It is especially within this RH range where liquid water exists in the wood structure and the relationships obtained can be used to determine the influence of this structure on water sorption (Siau 1995; Zhang and Peralta 1999).

The “ink-bottle effect” is also an important concept that needs to be considered for the interpretation of MC - ψ curves, especially at high ψ values. The capillary system of wood consists of cavities interconnected by narrow channels. The variation in dimensions between the different types of cavities connected in series suggests that desorption tends to

be governed by a lower water potential, which is determined by the narrower sections of the pores. In contrast, adsorption tends to be governed by a higher water potential, which depends on the larger sections of the pores; thus, the desorption isotherm will depend on the size of channels connecting the lumina, whereas the adsorption isotherm will depend on the size of these lumina (Fortin 1979). As a result, several works have reported a large hysteresis between the boundary desorption and adsorption curves for different wood species (Barkas 1936; Penner 1963; Fortin 1979), which has been principally attributed to the ink-bottle effect.

The mercury intrusion porosimetry (MIP) is commonly used for determining the characteristics of a porous media. MIP is a fast technique, but its results have to be considered with care (Roels et al. 2001). The mercury porosimetry does not measure the true distribution of pore sizes, but rather the pore entrance sizes. For instance, “ink bottle” pores are not characterized by the size of the bottle but by the neck, which leads to an overestimation of the fine pore volume and an underestimation of the wide pore volume (Delage and Lefebvre 1984; Roels et al. 2001). To apply MIP technique to wood, the anisotropic characteristic of this material has to be taken into account. In particular, the dimension of the sample in the longitudinal direction affects the results obtained by the MIP analyses. If a sample thickness is several times larger than the fiber length, a large quantity of wood elements will not be sectioned and the mercury is forced to pass through the channels connecting these elements (pits), in order to reach the lumina. This fact will influence the degree of penetration of mercury and will also produce the ink-bottle effect.

Trenard (1980) applied the MIP on beech wood samples having 240 μm and 10 mm in the longitudinal direction. The impregnation in the short samples was 46% larger than that in the long samples. The penetration of mercury was not complete even for samples 1mm thick. Mercury intrusion has also been used to evaluate the wood impregnability. Schneider (1983) and Hösli and Orfila (1985) used samples longer than the fiber length in order to reproduce the ink-bottle effect and to make the mercury impregnation analogous to the normal impregnation of wood with creosote. According to Fortin (1979), the water behavior within wood during drainage can be predicted by MIP results using samples thicker than the fiber length. The ink-bottle effect present in this case will act in the same way on a receding water meniscus as on an advancing mercury meniscus.

The pore size distribution can also be determined from sorption experiments obtained at high relative humidities. This method of determination has been applied for wood by several authors (Cloutier et Fortin 1991; Tremblay et al. 1996; Defo et al. 1999; Zhang and Peralta 1999); however, a comparison between the pore size distribution obtained by MIP and by sorption techniques has not been made before. The results obtained by these two techniques should be similar whether differences between them, for example, dimensions and MC of samples, are taken into account.

The purpose of this investigation was to evaluate the relationships between the wood porous structure and the EMC obtained in desorption at high values of RH. The EMC - ψ relationships of seven hardwood species were determined using two complementary sorption techniques. The results obtained were combined with a characterization of the wood structure by quantitative anatomical analyses, MIP essays and SEM images for all wood species.

5.4 Material and methods

Experiments were carried out with two temperate hardwoods: beech (*Fagus grandifolia* Ehrhart) and yellow birch (*Betula alleghaniensis* Britton); and five tropical hardwoods: cachimbo (*Cariniana domesticata* (C. Martius) Miers), congona (*Brosimum alicastrum* Swartz), huayruro (*Robinia coccinea* Aublet), pumaquiro (*Aspidosperma macrocarpon* C. Martius) and tornillo (*Cedrelinga cateniformis* Ducke). Twenty defect-free flat sawn boards of each wood species were carefully selected and stored in a conditioning room at 20°C and 60% RH. After conditioning, specimens were cut with a cross-section of 20 mm (R) by 20 mm (L) and a height of 60 mm (T). Matched samples were chosen from each board to make sorption tests, mercury porosimetry, and quantitative anatomical analyses. The average basic wood density (oven-dry mass to green volume) was 490 kg m^{-3} for tornillo (coefficient of variation (CV) of 3%); 533 kg m^{-3} for yellow birch (CV of 4 %); 540 kg m^{-3} for congona (CV of 4%); 543 kg m^{-3} for beech (CV of 3%); 550 kg m^{-3} for cachimbo (CV of 5%); 585 kg m^{-3} for pumaquiro (CV of 3%); and 639 kg m^{-3} for huayruro (CV of 3%).

For the mercury porosimetry tests, three of the twenty specimens for each species were chosen. For this, the lighter, the average and the denser specimen of each species were selected, which totaled 21 samples for this analysis. Wood blocks having a transverse

section of 1 cm by 1 cm were crosscut to 3.5 mm of thickness (L). The transverse faces of these blocks were then cut with a new microtome blade to a final thickness of 3 mm. This thickness was higher than the average fiber length of the woods studied, in such a way the ink-bottle effect could occur. Preliminary tests showed that samples with this thickness were almost fully mercury impregnated even though the ink-bottle effect was present. Such samples were put in a desiccator containing P_2O_5 and kept in anhydrous conditions until the tests.

For the quantitative anatomical analysis, twenty specimens of each wood species were used. Given the refractory character of some of the tropical woods used, wood blocks of 1 cm^3 were softened according to a method suggested by Kukachka (1977). After this treatment, microtome samples of transverse (20 μm thick) and tangential (30 μm thick) sections were prepared using a sliding microtome. The sections were then double stained with safranin and fast green, and mounted permanently.

EXPERIMENTS

Sorption tests

The sorption tests were performed in several desorption conditions for each species studied. Prior to the desorption tests, specimens were saturated in three steps (over KCl, over distilled water, and immersed in distilled water) until the full moisture content was reached. This was done in order to avoid internal defects caused by a rapid moisture adsorption (Naderi and Hernández 1997). A matched group of specimens was also tested at the full saturation condition. Item 2.4 gives a detailed description of the sorption procedure.

The sorption experiments were performed using two experimental techniques. The saturated salt solutions technique was applied between 33% and 90% RH. The pressure membrane procedure was used between 96.431% and 99.989% RH to determine points of longitudinal desorption. Table 3.1 gives details about the sorption tests. The pressure membrane technique is suitable for high RH conditions where equilibrium is mainly controlled by the capillary forces and consequently by the porous structure of wood. For this reason, the results of the second procedure will be discussed with more detail. The

relationship between water potential (ψ) and RH are shown in Table3.1. The water potential of moist air may be calculated from equation 2.1.

The radius of curvature of the air-water meniscus (r) is also presented in Table 3.1. This radius can be calculated from the relationship existing between the pressure applied on the sample side of a pressure membrane apparatus and the capillary structure of wood (Eq. 2.2).

According to Siau (1995), equation 2.2 is not applicable under about 92% RH, given that the radii becomes in the range or smaller than the water's molecular radius. Also, the mechanism of sorption appears to shift from a capillary sorption up to $\psi = -10^3$ Jkg^{-1} to a chemisorption, as ψ becomes lower than this ψ value.

For each point of desorption, twenty fully-saturated specimens were placed into a pressure extractor on a saturated cellulose acetate membrane. The time required to reach the equilibrium condition varied between seven and seventy days of desorption, depending on the ψ considered and the wood species tested.

As soon as each sorption test was completed, the mass of the sample was measured to the nearest 0.001g. This mass and that measured after oven drying were used to calculate the EMC, expressed as a percentage of oven-dry mass.

Mercury porosimetry analysis

According to Washburn (1921), the pressure required to force a non-wetting liquid (mercury) into a capillary pore is inversely proportional to the diameter of the capillary and directly proportional to the liquid surface tension and the contact angle between the porous material and the liquid. If it is assumed that the capillary is cylindrical and the opening of the transverse section is circular, the relationship between the applied pressure (P) and the pore size into which the mercury can penetrate is:

$$P = \frac{-2\gamma\cos\theta}{r} \qquad (5.1)$$

where: P is the applied pressure (Pa); γ is the surface tension of mercury (0.485 N m^{-1} at 20ºC); θ is the contact angle between the mercury and the surface of the capillary (130º); r is the pore radius (m).

As discussed later, the ink-bottle effect affects the pore size distribution obtained by the MIP technique. The results obtained from equation 5.1 are only an estimation of the pore size distribution of wood because of the assumption that pores are circular.

The MIP tests were carried out using a Micromeritics AutoPore IV. Low-pressure measurements were made from 0 to 345 kPa (pore radius from 180 μm to 1.8 μm) and high-pressure measurements were made from atmospheric pressure to 414 MPa (pore radius until 0.0015 μm). At the intrusion phase, about 80 cumulative pressure steps were applied, each of 10 seconds duration, for each specimen studied. Measurements of volume were kept within the range of 30% to 80% of the stem volume in order to remain within the maximum accuracy of the porosimeter.

Values of MIP were used to determine the pore volume distribution by pore size. This method also generates the envelope density (anhydrous density) and the skeletal density (cell wall density). The former is determined at the beginning of the test, when the mercury surrounds the sample. The skeletal volume of the sample is determined by increasing pressure and causing the mercury to invade all the open pore space. If, at the maximum pressure, all open pores in the sample are filled, then the volume of mercury intruded is equal to the pore volume. This value subtracted from the envelope volume of the sample yields its skeletal volume (Webb 2001).

Quantitative anatomical analysis

Two images of each sample were randomly taken using a Pixelink camera, for a total of 40 transverse images for the determination of vessels, fibers, and axial parenchyma parameters and 40 tangential images for determination of ray parameters of each wood species. Image treatments, based on objective criteria, were made using Micromorph 1.3 and Adobe Photoshop Elements 2.0. A Regent Instruments WinCell 2004 image analyzer was used to measure the quantitative anatomical parameters.

Several anatomical parameters were defined in order to evaluate their relationships with the boundary desorption curve of the seven wood species. The more important anatomical characteristics were as follows: vessel proportion (VP), tangential vessel diameter (VTD), smaller vessel diameter (VSD), larger vessel diameter (VLD), rays proportion (RP), rays

height (RH), rays width (RW), axial parenchyma proportion (APP), fiber proportion (FP), smaller diameter of fiber lumen (FSD) and larger diameter of fiber lumen (FLD). The axial parenchyma of tornillo was very difficult to be differentiated from the fibers in such a way that this parameter was determined on five samples only for this wood (instead of twenty).

5.5 Results and discussion

Mercury porosimetry results

The main results of the MIP tests are presented in Table 5.1. Cell wall anhydrous density values between 1 300 kg m^{-3} and 1 438 kg m^{-3} were obtained. Stayton and Hart (1965) also determined the cell wall density of three softwood species by the MIP method. To ensure the total penetration of mercury, a sample thickness of 320 μm was used and cell wall densities within the range of 1 440 kg m^{-3} to 1 450 kg m^{-3} were determined. In the present study, the sample thickness was 3 mm in order to have the presence of the bottle-ink effect. The lower values of cell wall densities obtained in the present work indicate that the overall penetration of mercury was not achieved for all wood species. This was probably the case for yellow birch, cachimbo, and tornillo woods (Table 5.1). As a result, the pore size distribution of these species was affected since a portion of the pore space remained unfilled by mercury. The results of anhydrous porosity (ε_o) confirm these findings. Thus, table 5.1 shows that the differences between ε_o obtained by the MIP technique and that calculated according to Siau (1995) were highest in the case of these three species.

The mean values of anhydrous density (G_o) from samples used for the MIP tests and for the sorption experiments are also shown in Table 5.1. In general, the mean of G_o from the three MIP samples was similar to that obtained from the twenty samples used in sorption tests. The highest differences were observed in congona and beech (27 kg m^{-3} and 17 kg m^{-3}, respectively). The differences in density can affect the comparison between the MIP results and those of sorption for such woods.

A typical cumulative pore size distribution for huayruro is shown in Figure 5.1. A large hysteresis between the intrusion and extrusion curves exists. This phenomenon has been

Table 5.1. Results of the mercury intrusion porosimetry for the seven hardwoods studied.

Wood species	Anhydrous density (kg m^{-3})		Cell wall density (kg m^{-3}) [3]	Anhydrous porosity (%)		Pore radius (μm) [5]
	$G_{o\ MIP}$ [1]	$G_{o\ sorption}$ [2]		$\varepsilon_{o\ MIP}$	$\varepsilon_{o\ calc}$ [4]	
Tornillo	554 (6.3) [6]	547	1 365 (2.3)	59.5 (3.1)	61.6	0.18; 0.04 [7]
Cachimbo	617 [8]	621	1 334	53.9	57.2	0.75
Yellow birch	632 (5.7)	624	1 300 (0.6)	51.4 (5.0)	56.2	0.44
Congona	640 (6.9)	613	1 409 (1.1)	54.6 (4.8)	55.7	0.32
Beech	672 (1.5)	655	1 414 (2.5)	52.4 (3.1)	53.4	20.30
Pumaquiro	672 (2.2)	668	1 399 (0.8)	51.9 (2.8)	53.4	30.51
Huayruro	727 (8.2)	732	1 438 (1.9)	47.8 (6.7)	49.6	0.04

[1] Density based on anhydrous mass and volume, determined during the test at 0.003 MPa.
[2] Density calculated from the average basic density (BD) of samples used on sorption tests.
[3] Cell wall density determined at maximum pressure (414 MPa), where all open pores with a pore radius larger than 0.0015 μm are filled.
[4] Anhydrous porosity to nonpolar liquids calculated by $\varepsilon_{ocalc} = 1 - (0.693 \times G_o)$ (Siau 1995).
[5] Pore radius where the volume of mercury penetrated into the sample was maximum (determined in the incremental intrusion curve).
[6] Values between parentheses represent the coefficient of variation, en percentage.
[7] Tornillo presented two pore radii with similar maximum volume of mercury penetrated into the samples.
[8] Results of cachimbo were based on two samples (lighter and denser samples).

ascribed to the ink-bottle effect and to the fact that the intrusion and withdrawal of mercury will be in general associated with a different group of pores. Thus, the threads of mercury tend to break and to leave globules trapped in many of the cavities. Another cause of hysteresis is that the contact angle may be different as the mercury is advancing over or receding from a solid surface (Gregg and Sing 1982). The large volume of mercury trapped within the wood sample after the mercury extrusion cycle confirms that the pore structure of wood is very complex, where a large amount of cavities are interconnected by narrow channels.

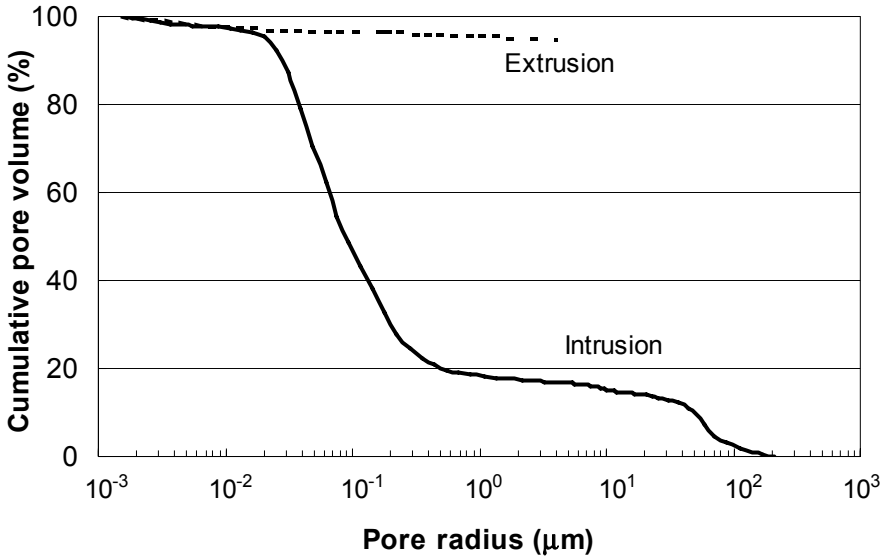

Figure 5.1. Cumulative pore size (intrusion and extrusion curves) for huayruro.

The results of the incremental mercury intrusion for the seven hardwoods studied are depicted in Figures 5.2A, 5.2C, 5.2E and 5.2G. This parameter represents the amount of mercury filled into each pore radius range, such that the peaks in the curves indicate the range of higher proportions of pore radius. These figures show a large pore structure variation among the wood species. The woods studied were grouped in these figures according to a similar pore structure. The largest mercury intrusion occurred at pore radius larger than 10 µm for beech and pumaquiro (Figure 5.2A); between 0.2 µm and 1 µm for cachimbo and congona (Figure 5.2C); and between 0.02 µm and 0.4 µm for tornillo and huayruro (Figure 5.2E). Finally, yellow birch wood showed various intrusion peaks in pore radius larger than 0.3 µm (Figure 5.2G). Such differences in the pore structure will markedly affect the sorption curves of these hardwoods.

The intrusion of mercury in beech wood (Figure 5.2A) is a good example of the similarities between MIP and anatomical results. This intrusion seems to start at a pore radius smaller than for the other wood species, with a maximum pore opening of 36.6 µm in diameter. This agrees with the quantitative anatomical analysis, which shows that beech wood presents the smallest tangential diameter of vessels among the species studied (40.3 µm, Table 5.2). Trenard (1980) studied MIP intrusion in beech (*Fagus* sp.) and also observed a population of pore diameters around 40 µm.

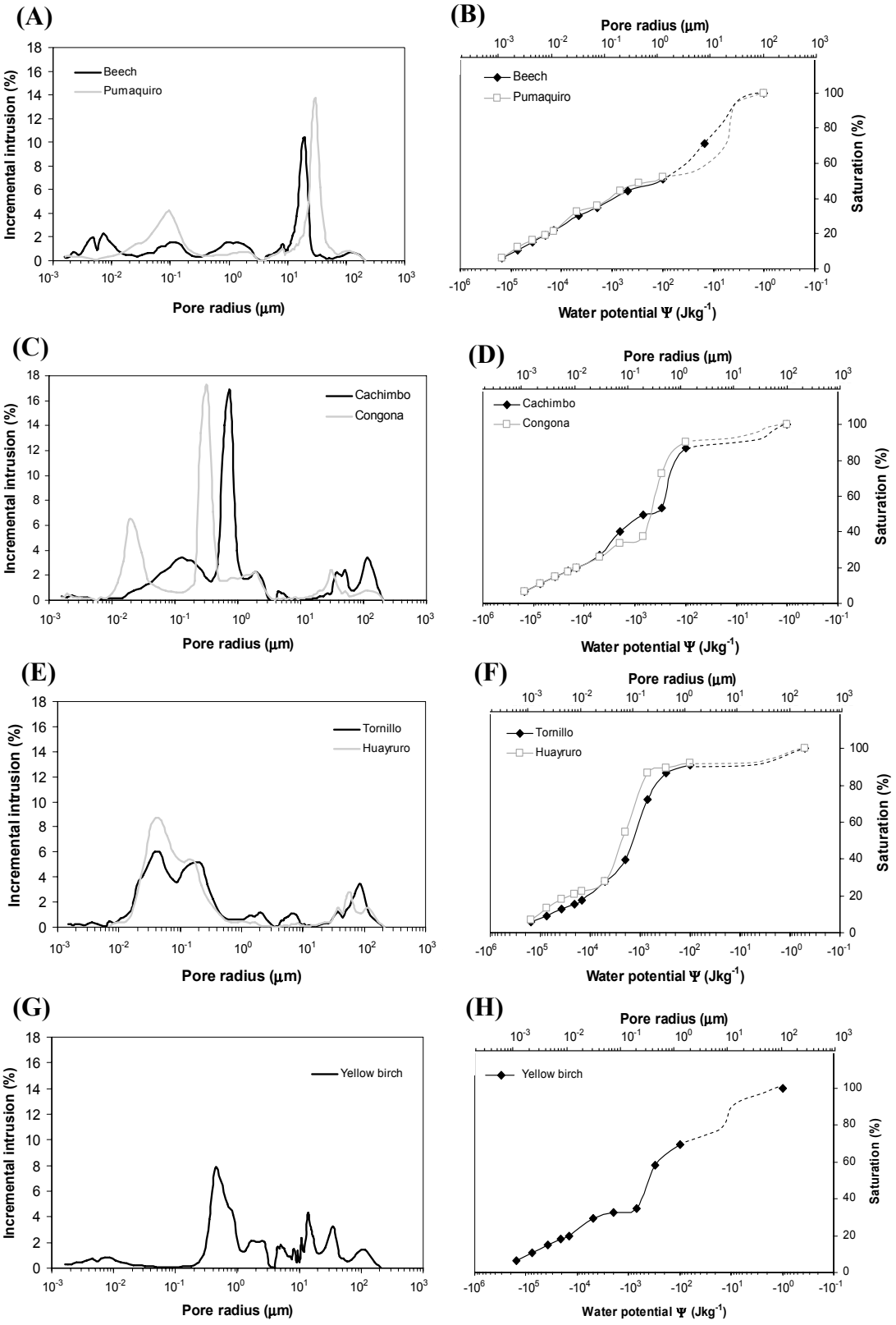

Figure 5.2. Incremental intrusion obtained by mercury porosimetry (A,C,E,G). Percent of moisture saturation-water potential relationship obtained by sorption tests (B,D,F,H). The discontinuous line between full saturation and -100 Jkg^{-1} ψ was adapted from mercury porosimetry measurements.

Interpretation of sorption curves using mercury porosimetry and anatomical analyses

The relationship between percent of moisture saturation and ψ of the seven wood species are shown in Figures 5.2B, 5.2D, 5.2F and 5.2H. The percent of saturation was used to eliminate differences in full saturation values among the wood species. This parameter is calculated as the ratio of water in wood (M_m-M_o) to the maximum water in wood (M_s-M_o), where M_m is the mass at a given moisture content, M_o is the oven-dry mass and M_s is the maximum mass at the full saturated condition, in percent (Choong and Tesoro 1989). Since the desorption was carried out beginning from full saturation, the term "boundary desorption curve" is used to describe this feature. The range between 96% and 100% RH is spread-out when using the water potential concept to represent sorption isotherms. This region is very important in the study of the wood-liquid water interactions, given that it is mainly controlled by the capillary forces and consequently by the structure of wood species. The results obtained by the saturated salt solution method are also shown for information purposes in Figure 5.2 only. These results, given that the capillary forces appear least important within the range of RH covered by this technique, are discussed in chapter 3. The same species grouped in the graphs presenting MIP results were also grouped in the sorption figures. Thus, a great similarity between the trends of these two experiments is observed. In particular, there is good agreement between the zones of higher porosity measured by the MIP technique and the range of ψ where an important loss of liquid water occurred. The great variation in drainage curves among the wood species can also be clearly observed (Figures 5.2B, 5.2D, 5.2F and 5.2H).

Concerning the similarities between MIP and sorption curves, one can observe the loss of liquid water in the first step of drainage (between full saturation and -100 Jkg^{-1} ψ) and the amount of mercury penetration into pore radius larger than 1.44 μm (Table 3.1 indicates that pore radii larger than 1.44 μm are already empty at this stage of desorption). Figure 5.2B shows that beech and pumaquiro presented the higher loss of percent of saturation in the first step of drainage (from 100% to 51% for beech and from 100% to 52% for pumaquiro). MIP results (Figure 5.2A) show that these species present the higher volume of pores with radius larger than 1.44 μm. The quantitative anatomical analyses of these species also corroborate these results. Beech and pumaquiro had the largest amount of

vessels (Table 5.2), which are the first drainage paths present in wood. Cachimbo and congona have a small proportion of vessels (Table 5.2), which explains the low loss of liquid water above -100 Jkg^{-1} ψ and the small mercury penetration at pores radius larger than 1.44 μm (Figures 5.2C and 5.2D). Table 5.2 shows that tornillo and huayruro also have a small quantity of vessels, which was reflected on the drainage curve of these species by a small loss of moisture in the beginning of the desorption (Figure 5.2F). The small proportion of mercury penetration at pores radius larger than 1.44 μm corroborate these results (Figure 5.2G).

Between full saturation and -300 Jkg^{-1} ψ for cachimbo and between full saturation and -700 Jkg^{-1} ψ for congona, the percent of saturation dropped from 100% to 54% for cachimbo and from 100% to 37% for congona (Figure 5.2D). In terms of mass units within a specimen, this corresponds to a loss of liquid water of 7.51 g for cachimbo and 10.28 g for congona. This water would have occupied a volume within the wood specimen of about 31% for cachimbo and 43% for congona (mean volume of the specimen at 12% EMC was 24 cm^3). The MIP results show that the proportion of wood pores larger than 0.48 μm (cachimbo) and 0.21 μm (congona) was of 36% for cachimbo and 37% for congona. The sum of the proportions of vessels, fiber lumina and axial parenchyma of cachimbo and congona were 35% and 38%, respectively. Thus, the proportion of the more permeable elements estimated by mercury porosimetry is very similar to the proportion of the vessels, fiber lumina and axial parenchyma obtained by the quantitative anatomical analysis. This fact corroborates the results obtained by Gonzalez and Siau (1978), who observed the impermeability of ray elements.

The boundary desorption curves depicted in Figure 5.2D indicate that the more important pore radius in desorption were in the range of 0.48 μm and 1.44 μm for cachimbo and between 0.21 μm and 1.44 μm for congona. The results of mercury intrusion are in agreement with such drainage curves. Figure 5.2C shows that the larger mercury intrusion was in the pore radius of 0.76 μm for cachimbo and 0.32 μm for congona. As stated earlier, the ink bottle effect is present in both curves (Figures 5.2C and 5.2D), which means that the drainage of fibers, axial and radial parenchyma is determined by the size of the pits connecting these elements. A typical SEM image of a fiber of congona (Figure 5.3A) shows

Table 5.2. Results of the quantitative anatomical analyses for the seven hardwoods studied.

Wood species	Volume of elements in wood (%)				Vessel tangential diameter (μm)	Larger diameter of fiber lumen (μm)	Smaller diameter of fiber lumen (μm)
	Vessel (VP)	Fiber (FP)	Axial parenchyma (APP)	Radial parenchyma (RP)			
Tornillo	8.4 (32.5)[1]	65.3 (6.4)	12.3 [2] (21.4)	14.0 (17.0)	255.3 (14.8)	15.9 (18.0)	10.3 (18.4)
Cachimbo	8.2 (42.6)	61.2 (10.5)	9.5 (18.5)	21.1 (18.2)	137.7 (8.8)	12.4 (14.8)	7.9 (17.0)
Yellow birch	15.3 (15.8)	74.0 (3.6)	0.4 (67.8)	10.3 (10.3)	86.2 (6.9)	13.5 (12.7)	8.4 (17.2)
Congona	6.5 (15.1)	71.0 (4.9)	5.3 (29.2)	17.2 (16.1)	94.9 (6.4)	8.5 (8.9)	5.6 (11.6)
Beech	24.9 (21.9)	59.9 (9.8)	3.3 (32.2)	11.9 (21.9)	40.3 (9.6)	6.0 (18.3)	3.5 (21.3)
Pumaquiro	28.3 (13.6)	59.3 (7.7)	3.2 (47.2)	9.2 (18.5)	90.3 (8.0)	9.7 (17.3)	5.3 (17.1)
Huayruro	5.2 (32.0)	41.2 (12.7)	33.5 (14.1)	20.1 (13.9)	171.9 (8.5)	4.2 (15.7)	2.6 (16.4)

[1] Values between parentheses represent the coefficient of variation based on 20 averages.
[2] APP of tornillo wood is based on 5 averages.

pit pore radius in the range of 0.2 μm and 0.6 μm. Nevertheless, the presence of the pit membrane decreases the effective pit opening. Figure 5.3B shows an axial parenchyma pit of congona, where the effective pit size opening is about 0.04 μm, which explains the intrusion of mercury in small pore radius. The large variation in the size of hardwood pit openings is manifested in the mercury intrusion results and, as a result, in the drainage curves of the different species.

The incremental intrusion curves of tornillo and huayruro showed that the largest proportion of the pore openings was within a radius range of 0.02 μm and 0.35 μm for tornillo and between 0.02 μm and 0.28 μm for huayruro (Figure 5.2E). This is perceived in the saturation curves (Figure 5.2F), where the principal drop was between -300 and -5 000 Jkg^{-1} ψ for tornillo and between -700 and -5 000 Jkg^{-1} ψ for huayruro. The great loss of liquid water could correspond to the drainage of the fibers and parenchyma elements. Cloutier and Fortin (1991) studied the pore size distribution in aspen wood and observed

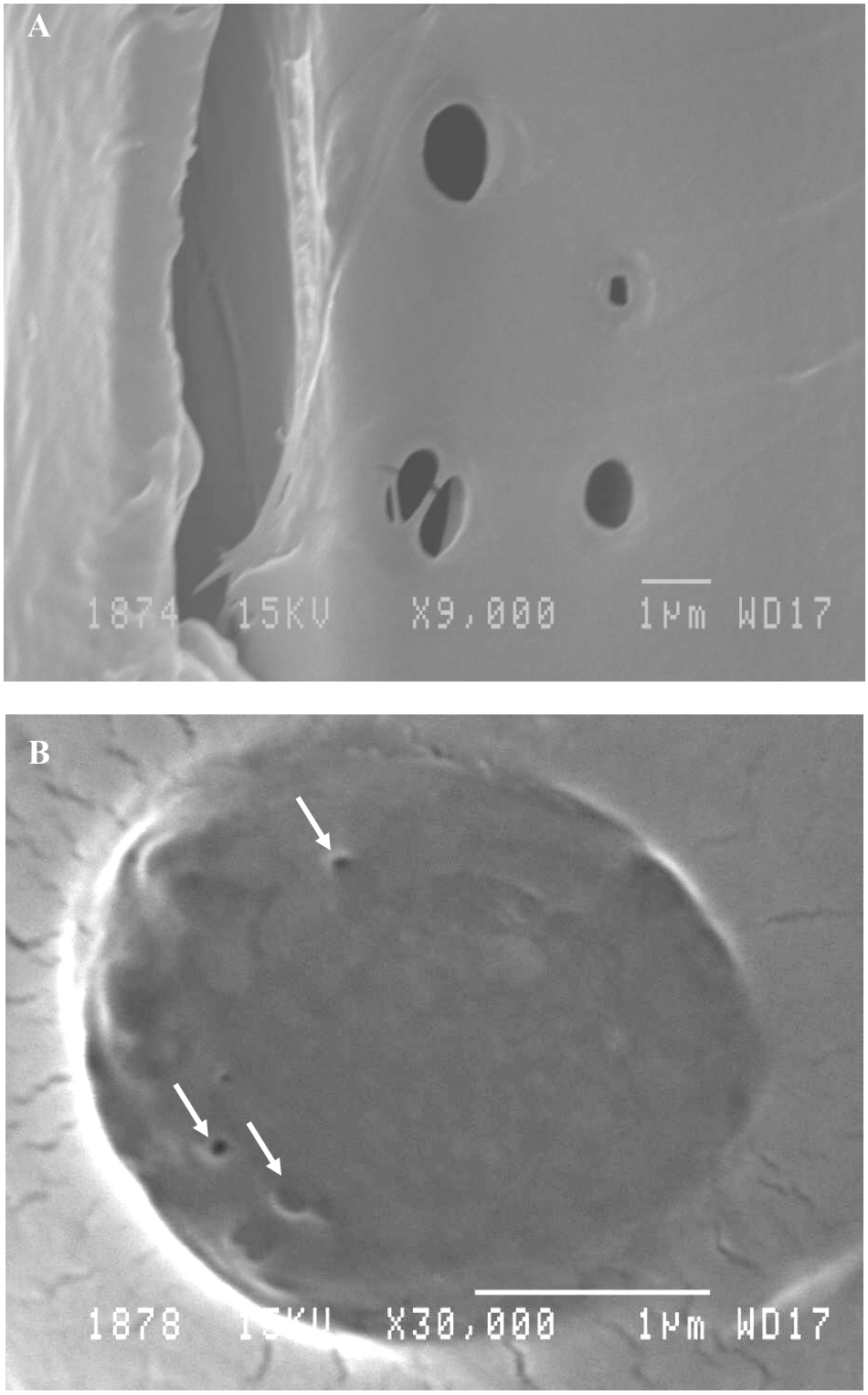

Figure 5.3. SEM images of pits. A) Fiber pits in congona. B) Axial parenchyma pit in congona showing the effective pit opening (arrows) of the pit membrane.

that a large proportion of the pore openings have a radius within 0.04 μm and 0.5 μm. The present work shows pore openings within the same magnitude and further extends the range of heterogeneity of the wood cavities.

As previously indicated, yellow birch presented a quite incomplete mercury impregnation, which affected cell wall density determination. This fact certainly affected the pore size distribution of this species. The incremental mercury intrusion curve of yellow birch can be divided in two groups of pore radius (Figure 5.2G). The first group corresponds to pore radius larger than 3 μm, which represents the vessels (average tangential radius of 43 μm, Table 5.2) and the cut fibers at the transverse faces of the specimens (average smaller radius of 4.2 μm, Table 5.2). The second group corresponds to the largest proportion of pore openings at about 0.4 μm, which is assumed to correspond to the penetration of fibers. It is also observed that 91% of mercury had already penetrated the wood in pore radius larger than 0.21 μm. Heizmann (1970) also observed for birch wood (*Betula verrucosa*) two groups of pore sizes, where the large proportion of pores had a radius of 0.7 μm and with another proportion between 2 μm and 4 μm. These zones observed by mercury porosimetry are manifest in the saturation curve (Figure 5.2H), where two drops are shown (one from full saturation to -100 Jkg^{-1} ψ, and another from -100 to -700 Jkg^{-1} ψ). The plateau observed below -700 Jkg^{-1} ψ (pore radius smaller than 0.21 μm) indicates that openings controlling the retention and flow of water are scarce below this ψ value. The water remaining in wood would be localized in capillaries having a radius equal to or smaller than about 0.072 μm (Table 3.1). This plateau would correspond to the transition between the drainage of the fiber cavities and that of the cell walls and ray parenchyma lumina. This liquid water remaining below -700 Jkg^{-1} ψ should be located in the least permeable wood elements, as suggested by Hart et al. (1974) and Hernández and Bizoň (1994).

As observed by Schneider (1983) and Hösli and Orfila (1985), mercury porosimetry can also be used to evaluate the wood impregnability. The curves of mercury incremental intrusion show that beech and pumaquiro woods presented pore openings with larger radii (Figure 5.2A). In contrast, tornillo and huayruro woods were the species with smaller pore openings (Figure 5.2E). During preparation for the sorption tests, beech and pumaquiro

woods were full saturated very easily, while tornillo and huayruro were more difficult to be full saturated. These results confirm that mercury porosimetry can also be used to predict the impregnability of wood.

Comparison of boundary drainage curves determined by sorption tests and MIP

As discussed previously, the intrusion results of mercury porosimetry might be used to determine the boundary water drainage in wood (Figure 5.2). Sorption experiments normally need long periods to reach equilibrium while MIP analysis requires only few hours. MIP results were then used to estimate the desorption curves at high RH values for the seven hardwood species. For this, the void volume determined by MIP for each class of pores was considered as corresponding to the same volume of liquid water emptied during desorption. The boundary desorption curves estimated by MIP results and those obtained by sorption tests are presented together in Figure 5.4 for comparison purposes.

An important difference between sorption and MIP methods is the moisture content of the samples prior to the tests. The porosity was based on the bulk volume at the anhydrous condition for MIP test and on the full saturation condition for the sorption test. According to Heizmann (1970), the MIP technique does not describe sufficiently the pore size distribution of wood at the swollen state, in particular for the pores below 0.2 μm in diameter.

The length of the sample was also different for the two methods (3 mm and 20 mm for mercury porosimetry and sorption methods, respectively). The sorption samples were several times longer than the fiber length, which should affect the pore size distribution obtained because of the ink-bottle effect. This will result in an overestimation of the volume of smaller pores on the sorption samples. As mentioned earlier, the vessels are generally the most important path of longitudinal flow. Petty (1978) studied flow through birch wood and observed that about 20% of the vessels are short enough to posses vessel endings within a sample of 20 mm. As a result, fluid flow of these vessels to adjacent vessels is only possible by intervascular pits (decreasing the effective pore opening). It is therefore clear that the number of vessel endings within the sample were higher in sorption samples than in MIP samples. On the other hand, the length of the sample will also affect

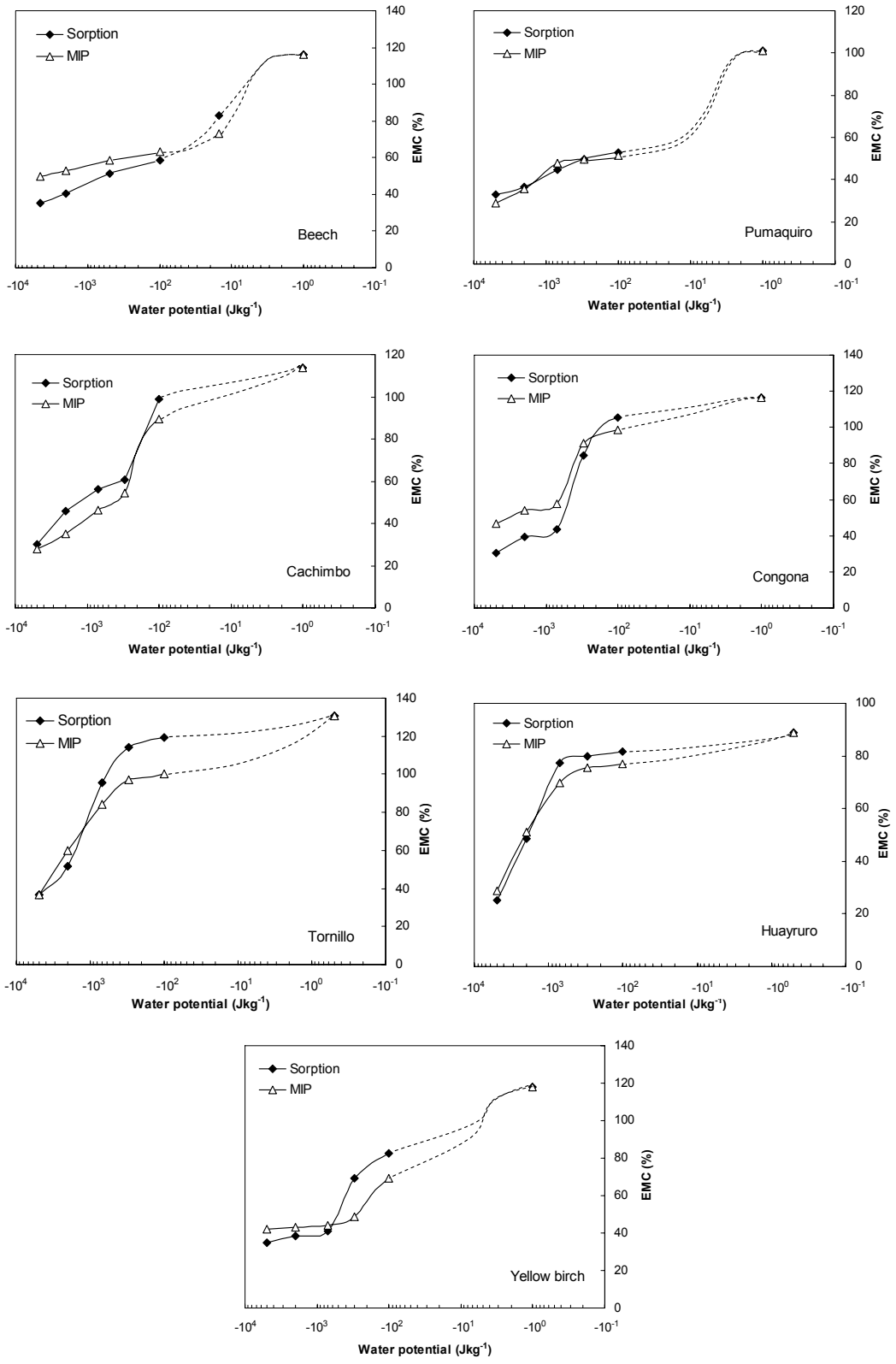

Figure 5.4. EMC - ψ relationships for the seven species studied along the boundary desorption curve obtained by sorption tests (25°C) and MIP analyses.

the proportion of open-cut elements on the sample surface. Thus, the proportion of cut elements was higher in MIP samples than in sorption samples.

Given that boundary curves deduced from MIP results only indicate the loss of liquid water; this fact must be considered in the comparison of the curves depicted in Figure 5.4. Thus, items 2.5 and 3.5 show that loss of bound water occurs at EMC values higher than the FSP. The proportion of volumetric shrinkage observed at early states of desorption (Hernández and Pontin 2006, and chapters 2-3) was used to estimate this loss of bound water. In order to compare MIP and sorption curves showed in Figure 5.4, this amount of bound water was corrected on the drainage curves estimated by MIP results.

The efficiency in the use of MIP results to the prediction of the boundary desorption curves varied among species (Figure 5.4). A very good agreement was obtained for pumaquiro and huayruro. The differences observed for the yellow birch, cachimbo and tornillo woods could be explained in part by the incomplete mercury intrusion reported for these species previously. For beech and congona, the differences in wood anhydrous density between MIP and sorption samples may also explain some deviations between the two curves. Thus, taking into account these considerations, it can be concluded that the boundary desorption curves estimated by the two methods had similar trends.

According to this discussion, it is evident that some important differences between sorption and MIP methods must be considered when analyzing the results, for example the moisture content and the size of the samples used. Also, the quantity of mercury penetrated into the wood sample will affect the accuracy of the results obtained. However, the MIP technique appears as a useful tool for the evaluation of the wood impregnability and for the prediction drainage behavior of wood in the region mainly governed by the capillary forces.

5.6 Conclusions

Sorption tests were performed in two temperate and five tropical hardwoods. Special attention was paid to the high relative humidity range where sorption is mainly governed by the capillary forces. The pore characteristics of these hardwoods were determined by mercury intrusion porosimetry (MIP) and by quantitative anatomical analyses in order to study the influence of the wood structure on its boundary drainage. MIP and quantitative

anatomical analyses gave similar results, principally for the vessel parameters. MIP was an important way to determine the pore size distribution of wood, permitting the prediction of the liquid water behavior in wood during boundary drainage. However, mercury porosimetry remains such a complex technique that several aspects must be considered in order to obtain useful information. The efficiency of mercury porosimetry to reproduce boundary drainage curves varied among species. Nevertheless, boundary drainage curves obtained by sorption tests and MIP showed similar trends for the species studied.